Useful Information from Axial Peak Magnetization in Projected NMR Experiments

T. Szyperski, D. Braun, B. Banecki, and K. Wüthrich*

Institut für Molekularbiologie und Biophysik
Eidgenössische Technische Hochschule-Hönggerberg
CH-8093 Zürich, Switzerland

Received March 27, 1996

Axial peaks arise from magnetization which is not frequency-labeled in at least one indirect dimension of a multidimensional NMR[1] experiment.[2] Because they correspond to incomplete coherence transfers, axial peaks represent a considerable magnetization reservoir. Here we show that the previously introduced projection technique[3,4] allows the derivation of useful information from axial coherences. In these experiments[3−15] the evolution of chemical shifts in the projected dimension gives rise to cosine modulation of the transfer amplitude, which leads to peak doublets encoding $n + 1$ chemical shifts in an n-dimensional spectrum. Axial single-quantum coherences which are frequency-labeled in all indirect dimensions except the projected one can be observed as peaks located at the center of the doublets. Simultaneous acquisition of projected and central peaks facilitates the symmetrization of the spectrum[6,9,16] and the unambiguous assignment of multiple peak doublets with degenerate chemical shifts in the other dimensions.[6,15]

NMR experiments delineating exclusively scalar connectivities are either "out-and-stay" experiments, in which excitation and detection is on different nuclei, or "out-and-back" schemes, in which the magnetization is detected on the same proton which was initially excited (Figure 1).[17] Moreover, the one-bond scalar coupling topology of the spins correlated in different indirect dimensions of out-and-back experiments (S, K, and L in Figure 1) may be bifurcated or linear. For "bifurcated out-and-back" 3D HS<KL> experiments, where underlined letters denote nuclei observed in a common dimension[4] and the enclosed spins represent the two branches, recording of central peaks can be achieved as recently described for 3D HNN<COCA>.[6] After magnetization transfer from H to S, $^1J_{SK}$ and $^1J_{SL}$ at the branching point (Figure 1a) evolve simultaneously, and the spin with the larger coupling to S is detected in quadrature. The product operator terms $S_xK_zL_z$ and S_yK_z give rise to doublets and central peaks, respectively, which have opposite sign (see Figure 4 in ref 6). In the corresponding 4D experiment, the term S_yK_z would give rise to noninformative axial peaks.

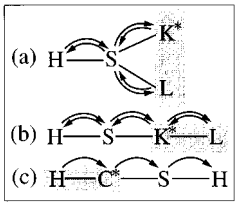

Figure 1. Magnetization transfer pathways of reduced-dimensionality triple-resonance experiments. (a) "Out-and-back" 3D HS<KL> experiment for bifurcated one-bond scalar coupling topology. (b) Corresponding 3D HSKL experiment for linear topology. (c) "Out-and-stay" 3D HCSH experiment. H and C denote proton and carbon spins, S a heterospin (*e.g.*, ^{13}C or ^{15}N), and K and L either protons or heterospins. The two nuclei observed in a common dimension are in a shaded box, and among these the nucleus detected in quadrature is marked with an asterisk. Uni- and bidirectional magnetization transfers are represented by arrows and double arrows, respectively.

Most triple-resonance pulse schemes designed for proteins[17] represent linear "out-and-back" experiments. In 3D HSKL (Figure 1b), $^1J_{SK}$ and $^1J_{KL}$ evolve during sequential transfer steps. Hence, central peaks have to come from magnetization which has been transferred to K, but not to L. With HSQC-type magnetization transfer and K detected in quadrature, the doublets and central peaks arise from the product operator terms $S_zK_zL_y$ and S_zK_y, respectively with peak patterns as in 3D HS<KL> (see supporting information). The transfer amplitudes of doublets and central peaks are proportional to $\sin^2(\pi^1J_{KL}\tau)$ and $\cos^2(\pi^1J_{KL}\tau)$, respectively, where τ is the duration of the transfer delay. Considering $^1J_{KL}$ only, all three peaks have the same intensity if $\cos^2(\pi^1J_{KL}\tau^\circ) = 0.5 \sin^2(\pi^1J_{KL}\tau^\circ)$ at $\tau^\circ = 0.61/(2^1J_{KL})$. τ° is close to the transfer maximum when rapid T_2-relaxation and/or additional passive couplings prevent a complete transfer. Then, the central peaks are exclusively derived from otherwise discarded magnetization and are acquired without extra expense of instrument time.

Projected 3D HCSH experiments rely on sequential in-phase magnetization transfer from ^{1}H *via* ^{13}C and S to ^{1}H (Figure 1c), so that magnetization initially excited on ^{1}H yields the doublets. When the refocusing delay of the first INEPT is set to a compromise value which accounts for simultaneous transfer from ^{1}H to ^{13}C in CH, CH_2 and CH_3,[18] a considerable fraction of ^{13}C single-quantum coherence originating from ^{13}C steady-state magnetization is not dephased by $^1J_{CH}$ at the end of this delay. If ^{13}C is detected in quadrature, this magnetization reservoir provides central peaks, while it would be discarded by axial peak suppression in the parent 4D experiment.[2] In the 3D $H^{\alpha/\beta}C^{\alpha/\beta}$(CO)NHN experiment,[5] which correlates the $^1H^{\alpha/\beta}$ and $^{13}C^{\alpha/\beta}$ chemical shifts of a given amino acid residue i in a protein with the backbone ^{15}N and $^1H^N$ chemical shifts of residue $i + 1$, the central peaks allow facile distinction of doublets from αCH and βCH by symmetrization about $\Omega(^{13}C^\alpha)$ and $\Omega(^{13}C^\beta)$, respectively. Considering $^1H^{\alpha/\beta}$ and $^{13}C^{\alpha/\beta}$ steady-state magnetization, the density matrix σ describing observable magnetization at the start of acquisition is proportional to[5,19 20]

(1) Abbreviations used: NMR, nuclear magnetic resonance; 2D, two-dimensional; 3D, three-dimensional; 4D, four-dimensional; HSQC, heteronuclear single-quantum coherence; γ(X), gyromagnetic ratio of nucleus X; DSS, 2,2-dimethyl-2-silapentane-5-sulfonate; 434(1−63), N-terminal 63-residue fragment of the 434 repressor.

(2) Ernst, R. R.; Bodenhausen, G.; Wokaun, A. *Principles of Nuclear Magnetic Resonance in One and Two Dimensions;* Clarendon Press: Oxford, 1987.
(3) Szyperski, T.; Wider, G.; Bushweller, J. H.; Wüthrich, K. *J. Biomol. NMR* **1993**, *3*, 127−132.
(4) Szyperski, T.; Wider, G.; Bushweller, J. H.; Wüthrich, K. *J. Am. Chem. Soc.* **1993**, *115*, 9307−9308.
(5) Szyperski, T.; Pellecchia, M.; Wüthrich, K. *J. Magn. Reson. B* **1994**, *105*, 188−191.
(6) Szyperski, T.; Braun, D.; Fernández, C.; Bartels, C.; Wüthrich, K. *J. Magn. Reson. B* **1995**, *108*, 197−203.
(7) Simorre, J. P.; Brutscher, B.; Caffrey, M. S.; Marion, D. *J. Biomol. NMR* **1994**, *4*, 325−333.
(8) Brutscher, B.; Simorre, J. P.; Caffrey, M. S.; Marion, D. *J. Magn. Reson. B* **1994**, *105*, 77−82.
(9) Brutscher, B.; Cordier, F.; Simorre, J. P.; Caffrey, M. S.; Marion, D. *J. Biomol. NMR* **1995**, *5*, 202−206.
(10) Brutscher, B.; Morelle, N.; Cordier, F.; Marion, D. *J. Magn. Reson. B* **1995**, *109*, 238−242.
(11) Löhr, F.; Rüterjans, H. *J. Biomol. NMR* **1995**, *6*, 189−197.
(12) Simorre, J. P.; Zimmermann, G. R.; Pardi, A.; Farmer, B. T.; Müller, L. *J. Biomol. NMR* **1995**, *6*, 427−432.
(13) Rexroth, A.; Schmidt, P.; Szalma, S.; Geppert, T.; Schwalbe, H.; Griesinger, C. *J. Am. Chem. Soc.* **1995**, *117*, 10389−10390.
(14) Bartels, C.; Xia, T.; Billeter, M.; Güntert, P.; Wüthrich, K. *J. Biomol. NMR* **1995**, *6*, 1−10.
(15) Morelle, N.; Brutscher, B.; Simorre, J. P.; Marion, D. *J. Biomol. NMR* **1995**, *5*, 154−160.
(16) Baumann, R.; Anil-Kumar; Ernst, R. R.; Wüthrich, K. *J. Magn. Reson.* **1981**, *44*, 76−83.
(17) Edison, A. S., Abildgaard, F.; Westler, W. M.; Mooberry, E. S.; Markley, J. *Methods Enzymol.* **1994**, *239*, 3−79.
(18) Burum, D. P.; Ernst, R. R. *J. Magn. Reson.* **1980,** *39*, 163−168.

S0002-7863(96)01015-3 CCC: $12.00

$$\sigma \sim I_{x,(i+1)} \cos[\Omega(^{15}N_{i+1})t_2]\{[1 - \exp(-T_{rel}/T_1(^1H^{\alpha/\beta}))] \sin[\pi^1 J_{CH}\tau] \cos^{(n-1)}[\pi^1 J_{CH}\tau] \cos[\Omega(^{13}C_i^{\alpha/\beta})t_1] \cos[\kappa\Omega(^1H_i^{\alpha/\beta})t_1] + \gamma(^{13}C)/\gamma(^1H)\,[1 - \exp(-T_{rel}/T_1(^{13}C^{\alpha/\beta}))] \cos^n[\pi^1 J_{CH}\tau] \sin[\Omega(^{13}C_i^{\alpha/\beta})t_1] \quad (1)$$

$I_{(i+1)}$ denotes H^N of residue $i + 1$ and τ the refocusing delay, $n = 1$, 2, or 3 for CH, CH_2, and CH_3, respectively, κ is the scaling factor for ^1H chemical shifts,[4,5] $T_1(X)$ and $\gamma(X)$ are the nonselective longitudinal relaxation time and the gyromagnetic ratio of nucleus X, and T_{rel} denotes the relaxation delay between successive scans, with $T_{rel} \gg \tau$. If ^{13}C is detected in quadrature, the first term of the sum in (eq 1) yields doublets along $\omega_1(^{13}C)$,[5] while the second term gives rise to central peaks. The central peaks are dispersive when the doublets are phased absorptive. To prevent cancellation from spectral overlap, we record two data sets in an interleaved fashion, between which the first 90° pulse on ^1H is shifted by 180°. Product operator terms from ^1H then have opposite sign, so that the sum and the difference yield two subspectra containing either the central peaks or the doublets. Addition of the subspectra is not recommended, since this would not facilitate the spectral analysis but decrease the signal-to-noise ratio[21] by $2^{1/2}$.

Figure 2 shows cross sections containing doublets (Figure 2a) and central peaks (Figure 2b) from a 3D $H^{\alpha/\beta}C^{\alpha/\beta}$(CO)NHN experiment with the uniformly ^{13}C,^{15}N doubly-labeled protein 434(1−63),[1,22] as well as the separation of the $\omega(^{13}C) \pm \Delta\omega(^1H)$ doublets by symmetrization about their centers (Figure 2, c and d). The fact that both spectra were derived from the same experiment ensured accurate relative positioning of the singlet and doublet peaks. At 13 °C, 434(1−63) reorients with a correlation time of about 6 ns (P. Luginbühl, K. Pervushin, H. Iwai, and K. Wüthrich, to be published), so that spectra of comparable quality can be expected for molecular weights up to about 15 kDa at commonly used temperatures around 30 °C.

τ (eq 1) was optimized for maximal intensity of the doublets, *i.e.*, for $^1J_{CH} = 135$ Hz, $\tau = 2.1$ ms.[5,20] Assuming that $[1 - \exp(-T_{rel}/T_1(^1H^{\alpha/\beta}))] = [1 - \exp(-T_{rel}/T_1(^{13}C^{\alpha/\beta}))]$ for small and medium-sized proteins,[23] and that INEPT provides the theoretical gain of $\gamma(^1H)/\gamma(^{13}C) = 4$, eq 1 predicts for CH, or for CH_2 with nondegenerate chemical shifts, that the ratios of the peak intensities of the doublet components and the corresponding central peaks are $2 \tan[\pi^1 J_{CH}\tau] = 2.47$. For CH_3 groups this number is 7.41. The actual values of these ratios are lowered by reduced INEPT gain and by $T_2(^1H)$-relaxation and passive $^1H-^1H$ scalar couplings during ^1H chemical shift evolution; we measured relative intensities of 1.9 ± 0.3 for 58 CH groups, 1.3 ± 0.3 for 41 CH_2 groups, and 3.9 ± 0.6 for 4 alanyl methyl groups in 434(1−63). Clearly, the central peaks will normally be observed when the doublets are recorded with a workable signal-to-noise ratio, and they may be present even if rapid $T_2(^1H)$-relaxation broadens the doublets beyond detection.

In conclusion, we propose the simultaneous acquisition of central peaks in reduced-dimensionality triple-resonance NMR experiments. Possible applications include 3D HNNCAHA (see supporting information), 3D HNNCOCA,[9] 2D HNNCA,[4] and 2D HNNCO[8] experiments recorded for small and medium-sized proteins, or 2D HCCH-COSY employed for ^{13}C labeled organic compounds, where for most experiments with macromolecules no additional investment of instrument time is required.

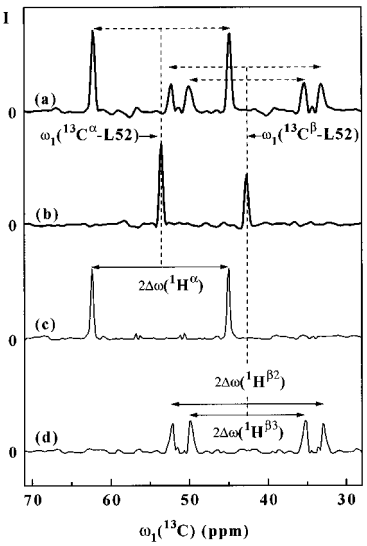

Figure 2. Cross sections along $\omega_1(^{13}C)$ taken from two subspectra of a 3D $H^{\alpha/\beta}C^{\alpha/\beta}$(CO)NHN experiment recorded on a Bruker AMX-600 spectrometer with acquisition of central peaks. The protein studied is the 434(1−63)[22] (T = 13 °C, pH = 4.6, concentration 2.5 mM). Chemical shifts are relative to internal DSS.[25] (a) Subspectrum containing the doublets of Leu 52 at $\omega_1(^{13}C^\alpha) \pm \Delta\omega_1(^1H^\alpha)$, $\omega_1(^{13}C^\beta) \pm \Delta\omega_1(^1H^{\beta 2})$, and $\omega_1(^{13}C^\beta) \pm \Delta\omega_1(^1H^{\beta 3})$, which are detected on the NH group of Gly 53 with $\omega_2(^{15}N) = 108.2$ ppm and $\omega_3(^1H^N) = 7.81$ ppm. (b) Subspectrum containing the corresponding central peaks at $\omega_1(^{13}C^\alpha)$ and $\omega_1(^{13}C^\beta)$. (c,d) Same as a after separation of the C^α and C^β doublets by symmetrization,[16] which was performed by replacing the intensities of each pair of data points i and j, centered about the maximum of the central peaks, by $\mathrm{sgn}(i)\cdot\min(i,j)$ in the case where i and j have the same sign and by zero otherwise. In a, c, and d, the in-phase splittings measured on the ^{13}C chemical shift scale in ppm, $2\Delta\omega_1(^1H)$, are equal to $2\kappa\,\delta\omega(^1H)[\gamma(^1H)/\gamma(^{13}C)]$, where $\delta\omega(^1H)$ denotes the chemical shift difference in ppm with respect to the ^1H carrier position at 2.96 ppm. The splittings are indicated by arrows. κ was set to 1.70, so that $\omega_1(^1H^\alpha) = 4.28$ ppm, $\omega_1(^1H^{\beta 2}) = 1.92$ ppm, and $\omega_1(^1H^{\beta 3}) = 1.58$ ppm. The $^{13}C^{\alpha/\beta}$ chemical shifts obtained from the central peaks in b are identified by dashed vertical lines at $\omega_1(^{13}C^\alpha) = 53.3$ ppm and $\omega_1(^{13}C^\beta) = 42.7$ ppm. The previously published pulse scheme for 3D $H^{\alpha/\beta}C^{\alpha/\beta}$ (CO)NHN[5] was supplemented with pulsed field gradients for coherence pathway rejection[26,27] and a sensitivity enhancement scheme,[28] and a semi-constant-time module[29] was used for ^1H frequency labeling. $82(t_1) \times 30(t_2) \times 512(t_3)$ complex points were accumulated; $t_{1,max}(^{13}C^{\alpha/\beta}) = 6.56$ ms, $t_{1,max}(^1H^{\alpha/\beta}) = 11.2$ ms, $t_{2,max}(^{15}N) = 21.0$ ms; $t_{3,max}(^1H^N) = 62.5$ ms. Two scans per increment were acquired, resulting in a measurement time of 22 h. The data matrix was extended by linear prediction[30] to 164 and 60 complex points along t_1 and t_2 and then multiplied with shifted sine functions. The spectrum was processed using the program PROSA.[32]

Acknowledgment. Financial support was obtained from the Schweizerischer Nationalfonds (Project 31.32035.91). We thank R. Marani for the careful processing of the manuscript.

Supporting Information Available: Figure with cross sections from a 3D HNNCAHA spectrum recorded for 434(1−63) with a pulse scheme derived from the experiment of Olejniczak[24] (3 pages). See any current masthead page for ordering and Internet access instructions.

JA961015T

(19) Grzesiek, S.; Bax, A. *J. Am. Chem. Soc.* **1992**, *114*, 6291−6293.
(20) Grzesiek, S.; Bax, A. *J. Magn. Reson.* **1992,** *99*, 201−207.
(21) Cavanagh, J.; Rance, M. *J. Magn. Reson.* **1990**, *88*, 72−85.
(22) Neri, D.; Wider, G.; Wüthrich, K. *FEBS Lett.* **1992**, *303*, 129−135.
(23) Wagner, G. *J. Biomol. NMR* **1993**, *3*, 375−487.
(24) Olejniczak, E. T.; Xu, R. X.; Petros, A. M.; Fesik, S. W. *J. Magn. Reson.* **1992**, *100*, 444−450.
(25) Wishart, D. S.; Bigam, C. G.; Yao, J.; Abildgaard, F.; Dyson, H. J.; Oldfield, E.; Markley, J. L.; Sykes, B. D. *J. Biomol. NMR* **1995**, *6*, 135−140.
(26) Wider, G.; Wüthrich, K. *J. Magn. Reson. B* **1993**, *102*, 239−241.
(27) Bax, A.; Pochapsky, S. S. *J. Magn. Reson.* **1992**, *99*, 638−643.
(28) Palmer, A. G.; Cavanagh, J.; Wright, P. E.; Rance, M. *J. Magn. Reson.* **1991**, *93*, 151−170.
(29) Grzesiek, S.; Bax, A. *J. Biomol. NMR* **1993**, *3*, 185−204.
(30) Stephenson, D. S. *Prog. Nucl. Magn. Reson. Spectrosc.* **1988**, *20*, 516−626.
(31) DeMarco, A.; Wüthrich, K. *J. Magn. Reson.* **1976**, *24*, 201−204.
(32) Güntert, P.; Dötsch, V.; Wider, G. and Wüthrich, K. *J. Biomol. NMR* **1992**, *2*, 619−629.